Phylogenetic analyses of trait evolution in Siphonophora (Cnidaria)

Catriona Munro[1]*, Stefan Siebert[1,2]*, Felipe Zapata[1,3], Mark Howison[4], Alejandro Damian Serrano[1,9], Samuel H Church[1,5], Freya Goetz[1,6], Phil Pugh[7], Steven H.D. Haddock[8], Casey W. Dunn[1,9]**

[1] Department of Ecology and Evolutionary Biology, Brown University, Providence, RI 02912, USA

[2] Current address: Department of Molecular & Cellular Biology, University of California at Davis, Davis, CA 95616, USA

[3] Current address: Department of Ecology and Evolutionary Biology, University of California Los Angeles, Los Angeles, CA 90095, USA

[4] Brown Data Science Practice, Brown University, Brown University, Providence, RI 02912, USA

[5] Department of Organismic and Evolutionary Biology, Harvard University, Cambridge, MA 02138, USA

[6] Current address: Smithsonian Institution, National Museum of Natural History, Washington, DC 20560, USA

[7] National Oceanography Centre, Southampton, SO14 3ZH, UK

[8] Monterey Bay Aquarium Research Institute, Moss Landing, CA 95039, USA

[9] Current address: Department of Ecology and Evolutionary Biology, Yale University, New Haven, CT 06520, USA

* Authors contributed equally

** Corresponding author, casey.dunn@yale.edu

Abstract

Introduction

Siphonophores (Fig. 1 and 2) are among the most abundant gelatinous predators in the open ocean, and have a large impact on ocean ecosystems (Williams and Conway, 1981; Purcell, 1981; Pugh, 1984; Pugh et al., 1997; Pagès et al., 2001; Choy et al., 2017). Siphonophores, which belong to Hydrozoa (Cnidaria), are found at all depths in the ocean. The most familiar species is the Portuguese man of war *Physalia physalis*, which floats at the surface and can wash up conspicuously onto beaches (Totton, 1960). Most species are planktonic, living in the water column, where some grow to be more than 30 meters in length (Mackie et al., 1987). There is also a small clade of benthic siphonophores, the Rhodaliidae (Pugh, 1983), that are tethered to the bottom for part of their lives. There are currently 188 valid described siphonophore species.

Siphonophores remain poorly known, in large part because they are fragile and difficult to collect. They have, however, been of great interest for more than 150 years in part due to their unique structure and development (Mackie et al., 1987; Mapstone, 2014). Like many other cnidarians, they are colonial: they grow by incomplete asexual reproduction. Each colony arises from a single embryo that forms the protozooid, the first body. One or two growth zones (Fig. 2) then arises that asexually produces other genetically identical zooids that remain attached (Carré, 1967, 1969; Carré and Carré, 1991, 1995). These zooids are each homologous to a solitary animal, but are physiologically integrated (Totton, 1965; Mackie et al., 1987; Dunn and Wagner, 2006). Siphonophores differ significantly from other colonial animals in colony structure, development, and the high degree to which their zooids are functionally specialized and arranged in precise, repeating, species-specific patterns (Beklemishev, 1969; Cartwright and Nawrocki, 2010). The functions that zooids are specialized for include feeding, reproducing, or swimming (Fig. 2) (Dunn and Wagner, 2006).

Understanding the unique ecology, morphology, and development of siphonophores requires a well-resolved phylogeny of the group. The relationship of siphonophores to other hydrozoans has been difficult to resolve (Cartwright et al., 2008; Cartwright and Nawrocki, 2010; Zapata et al., 2015), but there has been progress

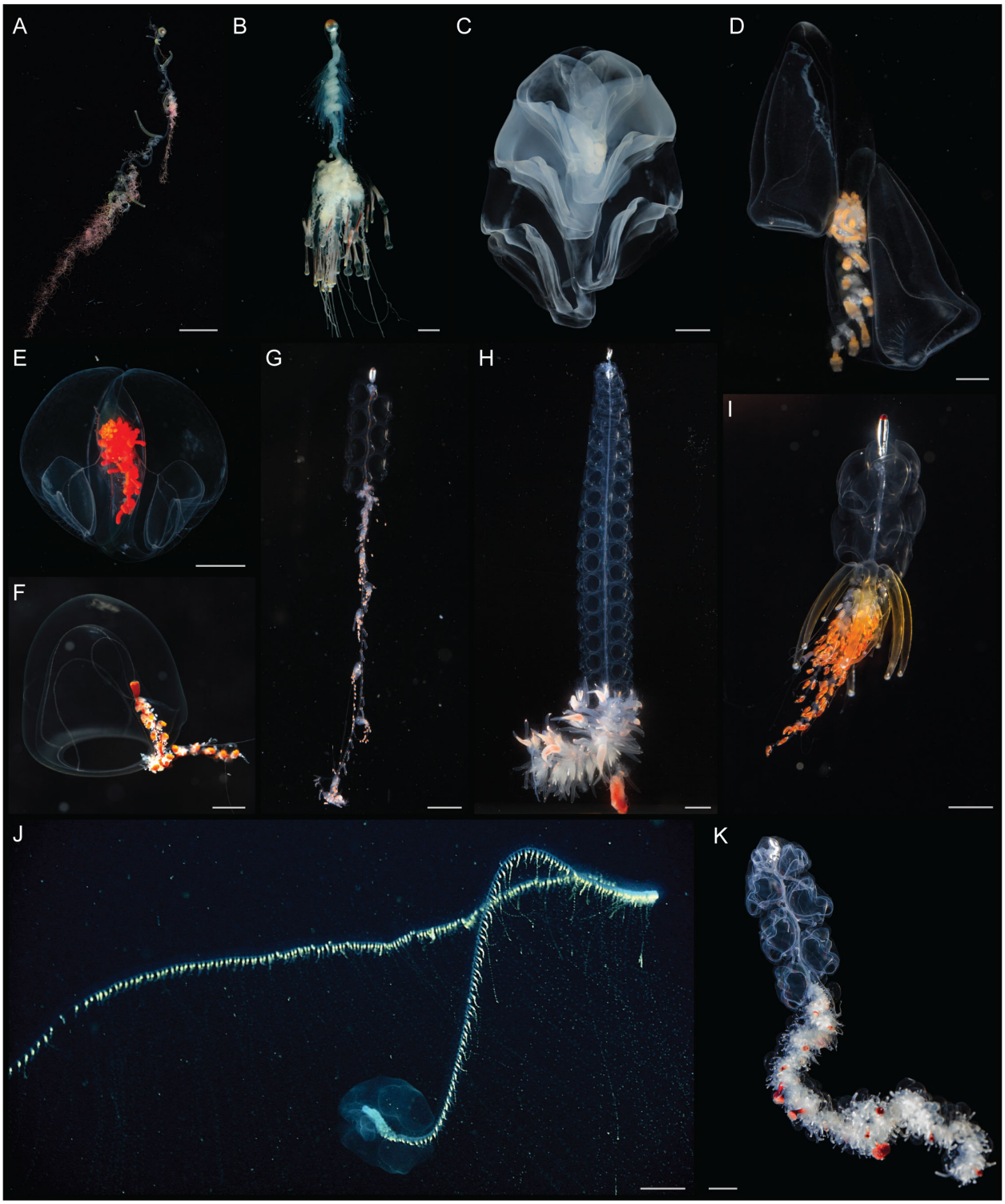

Figure 1: Photographs of living siphonophores. They correspond to the clades shown in Figure 3 as follows: Cystonectae (A-B), Calycophorae (C-F, J), Clade A within Euphysonectae (G-I) and Apolemiidae (K). (A) *Rhisophysa eysenhardtii*, scale bar = 1 cm. (B) *Bathyphysa conifera*, scale bar = 2cm. (C) *Hippopodius hippopus*, scale bar = 5 mm. (D) *Kephyes hiulcus*, scale bar = 2 mm. (E) *Desmophyes haematogaster*, scale bar = 5 mm. (F) *Sphaeronectes christiansonae*, scale bar = 2 mm. (G) *Nanomia bijuga*, scale bar = 1 cm. (H) *Lychnagalma utricularia*, scale bar = 1 cm. (I) *Physophora hydrostatica*, scale bar = 5 mm. (J) *Praya dubia*, scale bar = 4 cm . (K) *Apolemia* sp., scale bar = 1 cm.

on their internal relationships. A phylogeny (Dunn et al., 2005) based on two genes (16S, 18S) from 52 siphonophore taxa advanced several long standing questions about siphonophore biology. These include the relationships of the three historically recognised groups, Cystonectae, Physonectae, and Calycophorae. The Cystonectae was found to be sister to all other siphonophores, while the Calycophorae were nested within "Physonectae". The name Codonophora was given to this clade of "Physonectae" and "Calycophorae" (Dunn et al., 2005).

Major questions remained after this early work, though. There was, in particular, little support for important deep relationships within Codonophora. Understanding these relationships is key to resolving the evolution of several traits of importance, including sexual systems (monoecy versus dioecy) and the gain and loss of particular zooids, such as palpons (Fig. 2). Here we present a broadly sampled phylogenetic analysis of Siphonophora that considers transcriptomic data from 33 siphonophore species and 10 outgroup species (2 outgroups were subsequently excluded due to poor sampling). Using 1,071 genes, we find strong support for many relationships found in the earlier phylogeny (Dunn et al., 2005), and also provide new resolution for key relationships that were unresolved in that previous study. Using this phylogeny, we reconstruct the evolutionary history of characters central to the unique biology of siphonophores, including zooid type, life history traits, and habitat.

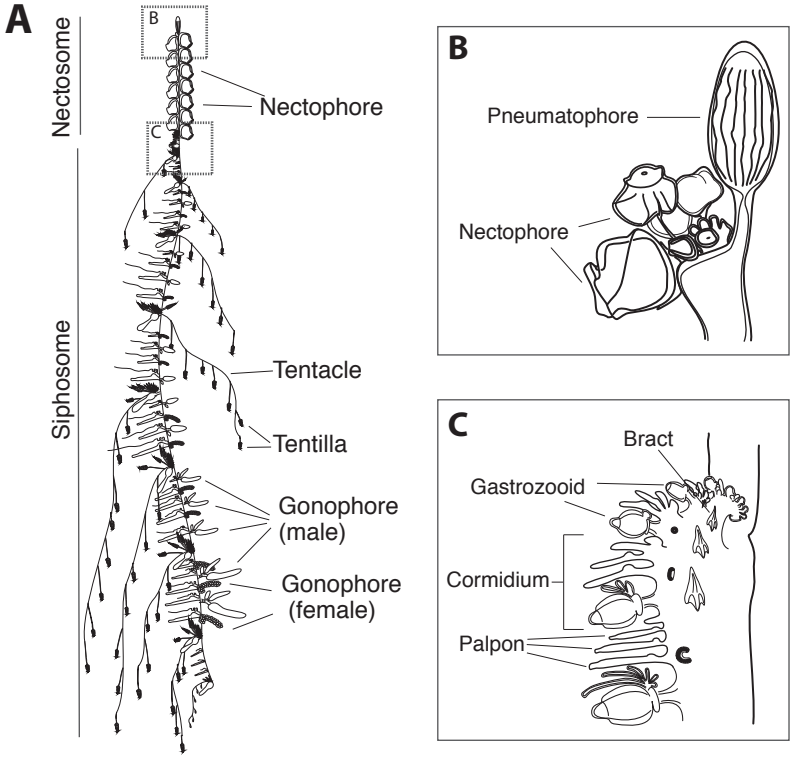

Figure 2: Schematic of the siphonophore *Nanomia bijuga*, orientated with the anterior of the colony at the top of the page, and the ventral side to the left. Adapted from http://commons.wikimedia.org/wiki/File:Nanomia_bijuga_whole_animal_and_growth_zones.svg, drawn by Freya Goetz. (A) Overview of the whole mature colony. (B) Inset of the pneumatophore and nectosomal growth zone. A series of buds gives rise to nectophores. (C) Inset of the siphosomal growth zone. Probuds subdivide to give rise to zooids in repeating-units (cormidia). The gastrozooid is the posterior-most zooid within each cormidium.

Methods

All scripts for the analyses are available in a git repository at https://github.com/caseywdunn/siphonophore_phylogeny_2017. The most recent commit at the time of the analysis presented here was 2d880de520609d7fe85ce1d366bce418e23c276b.

Collecting

Specimens were collected in the eastern Pacific Ocean, Mediterranean, and the Gulf of California. Collection data on all examined specimens, a description of the tissue that was sampled from the colony, collection mode, sample processing details, mRNA extraction methods, sequencing library preparation methods, and sequencing details are summarized in the file Supplementary data 1. Monterey Bay and Gulf of California specimens were collected by remotely operated underwater vehicle (ROV) or during blue-water SCUBA dives. *Chelophyes appendiculata* and *Hippopodius hippopus* specimens were collected in the bay of Villefranche-sur-Mer, France, during a plankton trawl on 13 April 2011. Available physical vouchers have been deposited at the Museum of Comparative Zoology (Harvard University), Cambridge, MA, the Peabody Museum of Natural History (Yale University), New Haven, CT, or had been previously deposited at the United States National Museum (Smithsonian Institution), Washington, DC. Accession numbers are given in Supplementary data 1. In cases where physical vouchers were unavailable we provide photographs to document species identity (see git repository).

Sequencing

When possible, specimens were starved overnight in filtered seawater at temperatures close to ambient water temperatures at the time of specimen collection. mRNA was extracted directly from tissue using a variety of methods (Supplementary data 1): Magnetic mRNA Isolation Kit (NEB, #S1550S), Invitrogen Dynabeads mRNA Direct Kit (Ambion, #61011), Zymo Quick RNA MicroPrep (Zymo #R1050), or from total RNA after Trizol (Ambion, #15596026) extraction and through purification using Dynabeads mRNA Purification Kit (Ambion, #61006). In case of anticipated very small total RNA quantities, only a single round of bead purification was performed. Extractions were performed according to the manufacturer's instruction. All samples were DNase treated (TURBO DNA-free, Invitrogen #AM1907;or on column DNase treatment with Zymo Quick RNA MicroPrep). Libraries were prepared for sequencing using the Illumina TruSeq RNA Sample Prep Kit (Illumina, #FC-122-1001, #FC-122-1002), the Illumina TruSeq Stranded Library Prep Kit (Illumina, #RS-122-2101) or the NEBNext RNA Sample Prep Master Mix Set (NEB, #E6110S). We collected long read paired end Illumina data for *de novo* transcriptome assembly. In the case of large tissue inputs, libraries were sequenced separately for each tissue, subsequently subsampled and pooled *in silico*. Libraries were sequenced on the HiSeq 2000, 2500, and 3000 sequencing platforms. Summary statistics for each library are given in the file Supplementary data 2. All sequence data have been deposited in the NCBI sequence read archive (SRA) with accession number XXX.

Analysis

New data were analysed in conjunction with 13 publicly available datasets, with a total number of 43 species. Sequence assembly, annotation, homology evaluation, gene tree construction, parsing of genes trees to isolate orthologous sequences, and supermatrix construction were conducted with Agalma v. 1.00 (Dunn et al., 2013; Guang et al., 2017). This workflow integrates a variety of existing tools (Grabherr et al., 2011, Altschul et al. (1990), Enright et al. (2002)„ Sukumaran and Holder (2010), Langmead and Salzberg (2012), Li and Dewey (2011), Talavera and Castresana (2007), Li et al. (2009), Katoh and Standley (2013)) and new methods. Maximum likelihood analyses of the supermatrix were conducted with RAxML v 8.2.0 (Stamatakis, 2006) and implemented via Agalma. Bayesian Inference (BI) analyses of the supermatrix were conducted using Phylobayes v. 1.7a-mpi (Lartillot et al., 2009). Sequence alignments, sampled and consensus trees, and voucher information are available in the git repository. Tree figures were rendered with ggtree (Yu et al., 2016).

Two outgroup species, *Atolla vanhoeffeni* and *Aegina citrea*, were removed from the final supermatrix due to low gene occupancy (gene sampling of 20.8% and 14.5% respectively in a 50% occupancy matrix with 2,203 genes). The final analyses presented here consider 33 siphonophore species and 8 outgroup species. This includes new data for 30 species. In the final analyses, we sampled 1,071 genes to generate a supermatrix with 60% occupancy and a length of 378,468 amino acids (Fig. S1).

ML analyses were conducted on the unpartitioned supermatrix using the WAG+Γ model of amino acid substitution, and bootstrap values were estimated using 1000 replicates. BI was conducted using two different CAT models, CAT-Poisson and CAT-GTR (Lartillot and Philippe, 2004). Two independent MCMC chains were run under the CAT-GTR model, and four independent MCMC chains were run under the CAT-Poisson model. The BI analyses did not converge (CAT-Poisson: maxdiff=1, meandiff=0.0148; CAT-GTR: maxdiff=1, meandiff=0.0127). Only the results from the CAT-Poisson model are presented here.Visual inspection of the traces indicated that a burn in of 400 trees was sufficient for all CAT-Poisson runs. This left 15847 trees in the posterior.

We used the Swofford-Olsen-Waddell-Hillis (SOWH) test (Swofford et al., 1996) to evaluate two hypotheses (Fig. 3C, S2): (i) "Physonectae" is monophyletic (Totton, 1965); (ii) monoecious species are monophyletic (Dunn et al., 2005). As the sexual system of *Rudjakovia* sp. is unclear, we carried out two tests of the monophyly of monoecy, one with *Rudjakovia* sp. included as a monoecious species, and one without (Fig. S2). We used SOWHAT (Church et al., 2015a) dev. version 0.39 (commit fd68ef57) to carry out the SOWH tests in parallel with the default options and an initial sample size of 100 (analysis code can be found in the git repository). For each hypothesis we defined a topology with a single constrained node that was inconsistent with the most likely topology (Fig. 3). We used a threshold for significance of 0.05 and following the initial 100 samples, we evaluated the confidence interval around the p-value to determine if more samples were necessary.

Morphological character data used in trait mapping were obtained from the literature or direct observation of available voucher material. Depth distribution data was queried from the MBARI VARS database (http://www.mbari.org/products/research-software/video-annotation-and-reference-system-vars/) (Schlining and Stout, 2006). We used stochastic character mapping to infer the probable evolution of traits on the tree in R using the `phytools` package (Huelsenbeck et al., 2003; Revell, 2012). Subsequent analyses were conducted in R and integrated into this manuscript with the `knitr` package. See Supplementary Information for R package version numbers.

Results and Discussion

Species phylogeny and hypothesis testing

Most relationships received strong support across analysis methods (Fig. 3A), with a couple of localized exceptions (Fig. 3B). The phylogenetic relationships recovered in this study are largely consistent with those found in a previous study based on two genes (16S and 18S ribosomal RNA) (Dunn et al., 2005). Relationships that receive strong support in both studies include the placement of Cystonectae as sister to Codonophora (the clade that includes all other siphonophores), the placement of Apolemiidae as sister to all other codonophorans, and the placement of Calycophorae within the paraphyletic "Physonectae". Multiple nodes that were not resolved in the previous two-gene analysis receive strong support in the present 1,071-gene transcriptome analyses. There is strong support for Pyrostephidae as sister to all other non-apolemiid codonophorans. Within the clade that is sister to the Pyrostephidae, we find two main clades, Calycophorae and a clade we here name Euphysonectae (Fig. 3A). It includes the remaining non-apolemiid, non-pyrostephid "Physonectae". We define Euphysonectae as the clade consisting of *Agalma elegans* and all taxa that are more closely related to it than to *Diphyes dispar*.

Euphysonectae consists of two reciprocally monophyletic groups we here provisionally refer to as Clade A and Clade B (Fig. 3A). Clade A is a group of siphonophores that all have an involucrum, or fold, that forms around the base of the cnidoband (Totton, 1965). This clade also shares the prescence of a descending mantle canal within the nectophores (Fig. S6), and is also monoecious (Fig. 5). Within Clade B there is low support

New data	Species	SRA Number	Depth (m)	Lat Lon
	Agalma elegans		3-20	35.56 N 122.55 W
Y	Bargmannia elongata		412/805/636/818	36.12 N 122.67 W
Y	Frillagalma vityazi		407	36.69 N 122.05 W
Y&N	Nanomia bijuga		414/387	36.60 N 122.15 W
	Physalia physalis	SRS431081		
	Abylopsis tetragona	SRX288276		
	Aegina citrea	SRS893439		
	Aiptasia pallida	SRX231866		
	Alatina alata	SRS893440		
Y	Apolemia rubriversa		767	36.70 N 122.05 W
	Atolla vanhoeffeni	SRS893451		
Y	Chelophyes appendiculata		3-20	
Y	Chuniphyes multidentata		327	36.79 N 122.00 W
	Clytia hemisphaerica			
Y	Cordagalma sp		252	36.70 N 122.06 W
	Ectopleura larynx	SRX315375		
Y	Erenna richardi		1044	36.61 N 122.38 W
Y	Forskalia asymmetrica		253	36.80 N 122.00 W
Y	Hippopodius hippopus		3-20	43.69 N 7.315 E
	Hydra magnipapillata			
	Hydractinia symbiolongicarpus	SRX474878		
Y	Kephyes ovata		452	36.36 N 122.81 W
Y	Lilyopsis fluoracantha		320	36.69 N 122.04 W
Y	Lychnagalma utricularia		431	36.69 N 122.04 W
Y	Marrus claudanielis		1427	36.07 N 122.29 W
	Nematostella vectensis			
Y	Physonect sp		1463	36.70 N 122.57 W
Y	Podocoryna carnea			
Y	Prayidae D27SS7		1363	35.48 N 123.64 W
	Prayidae D27D2	SRX288432		
Y	Resomia ornicephala		322	35.48 N 123.86 W
Y	Rhizophysa filiformis		10	27.23 N 110.46 W
Y	Stephalia dilata		3074	35.62 N 122.67 W
Y	Apolemia lanosa		1073	36.70 N 122.08 W
Y	Apolemia sp		461	36.60 N 122.15 W
Y	Bargmannia amoena		1251	36.70 N 122.08 W
Y	Bargmannia lata		1158	36.067 N 122.30 W
Y	Rudjakovia sp		334	36.00 N 122.42 W
Y	Thermopalia sp		3255	36.39 N 122.67 W
Y	Physophora gilmeri		242	36.36 N 122.40 W
Y	Halistemma rubrum		313	24.68 N 109.90W
Y	Athorybia rosacea		3-20	22.92 N 108.36 W
Y	Diphyes dispar		3-20	35.93 N 122.93 W

Table 1: Table 1. A complete list of specimens collected for this work. New data indicated by Y, blank fields indicate that data are already published.

for the placement of *Erenna richardi*, which is placed as sister to Clade A in some analyses (Fig. 3B). More taxon sampling will be required to determine the relationship of species within this clade.

Within Clade A, *Physophora gilmeri* along with *Lychnagalma utricularia* (both not included in the previous phylogeny) are sister to the Agalmatidae, a clade restricted to *Agalma*, *Athorybia*,*Melophysa*, *Halistemma* and *Nanomia* (Dunn et al., 2005; Pugh, 2006). In the rDNA study, *P. hydrostatica* (the presumed sister species to *P. gilmeri*) was sister to the Forskaliidae with low support. The position of *Cordagalma cordiforme* (= *Cordagalma ordinatum*) (Pugh, 2016) was previously unresolved, while in this analysis *Cordagalma* sp. is in a clade with *Forskalia asymmetrica*, falling outside of the Agalmatidae. Placement of *Cordagalma* outside Agalmatidae is consistent with previous analyses of morphological and molecular data (Dunn et al., 2005; Pugh, 2006).

Within Calycophorae, taxon sampling is shallower here than in the previous study. The calycophoran relationships that can be investigated, however, are in broad agreement with the previous analysis. Calycophorans have in the past been split into two groups, prayomorphs and diphyomorphs, based on morphology after Mackie et al. (1987). As in the previous study, the results presented here indicate that the prayomorphs are paraphyletic with respect to the diphyomorphs. *Craseoa lathetica* and *Desmophyes* sp. are sister to

Hippopodius hippopus in this study, while in the previous study, the relationship between *C. lathetica* and the clade including *H. hippopus* was unresolved.

Using the Swofford-Olsen-Waddell-Hillis (SOWH) test (Swofford et al., 1996), we evaluated the following three alternative phylogenetic hypotheses against the most likely tree topology (Fig. 3C): (i) monophyletic Physonectae, (ii) monophyletic monoecious siphonophores (both with and without *Rudjakovia* sp.). In all three tests the alternative hypothesis was rejected (p-value <0.01, confidence interval: <0.001 - 0.03, Fig. S2).

The broad sampling approach of this phylogeny provides new evidence for the relationships between major siphonophore clades within Codonophora, specifically between Pyrostephidae, Calycophorae, and the newly named Euphysonectae. This opens up new questions about key relationships within both Calycophorae and Euphysonectae – where future transcriptome sampling efforts should be focussed. Within Euphysonectae, two clades (Clade A and Clade B) are hypothesized, however there is weaker support for Clade B (Fig. 3A, 3B). Expanding sampling of species that probably fall in Clade B, including other *Erenna* species, rhodaliids, and relatives of Undescribed sp L, will greatly expand our understanding of these two groups and perhaps provide evidence of Clade B synapomorphies. Similarly, within Calycophorae, increased taxon sampling is needed. This study, and the previous study, suggest that the prayomorphs are paraphyletic, but for slightly different reasons. In Dunn et al. (2005), a clade of prayomorphs including *Praya dubia*, *Nectadamas diomedeae*, and *Nectopyramis natans* (not included in this study) were found to be sister to all other calycophorans, while in this study, the prayomorph *Lilyopsis flyoracantha* (not included in the previous study) is found in a clade including diphyomorph calycophorans that is sister to all other prayomorphs. Expanded taxon sampling, particularly *P. dubia* or a nectopyramid, but also extensive sampling across the major prayomorph and diphyomorph groups, will expand our understanding of relationships within Calycophorae. This will be especially important for understanding trait evolution within Calycophorae, for example, the release of eudoxids (Fig. 4), or the arrangement of male and female zooids along the stem (see below).

Character Evolution

Evolution of Monoecy

In all siphonophores, each gonophore (sexual medusa that produces gametes) is either male or female. Within each siphonophore species, colonies are either monoecious (male and female gonophores are on the same colony) or dioecious (male and female gonophores are on different colonies). Previous analyses suggested that the common ancestor of siphonophores was dioecious, and was consistent with a single gain of monoecy within the Codonophora and no secondary losses (Dunn et al., 2005). The better-resolved tree in the current analyses indicates that the evolution of monoecy is more complicated than this. The two clades of monophyloetic siphonophores, Calycophorae and Clade A (Fig. 3A), do not form a monophyletic group. This is because Clade B, which contains dioecious species, is also descened from their most recent common ancestor. SOWH tests strongly reject the placement of the monecious clades Calycophorae and Clade A as a group that excludes Clade B (Figs. 3C and S2). The positions of the only two taxa from Clade B in the previous analysies (Dunn et al., 2005), *Erenna* and *Stephalia*, were unresolved in that previous study. This difference in conclusions regarding trait evolution therefore does not reflect a contradication between alternative strongly supported results, but the resolution of earlier polytomies in a way that indicates there has been homoplasy in the evolution of monoecy.

The distribution of monoecy is consistent with two scenarios. In the first, there is a single shift from dioecy to monoecy along the branch that give rise to the most recont common ancestor of Calycophorae and Euphysonectae, followed by a shift back to dioecy along the branch that gave rise to Clade B. In the second, monoecy arose twice – once along the branch that gave rise to Clade A and again along the branch that gave rise to Calycophorae.

Ancestral character state reconstructions favor the hypothesis that monoecy arose twice (Fig. 5A), once in Calycophorae and once in Clade A. This is consistent with differences in the arrangements of male and female gonophores in the two clades. In Clade A, male and female zooids are found within the same cormidium. In

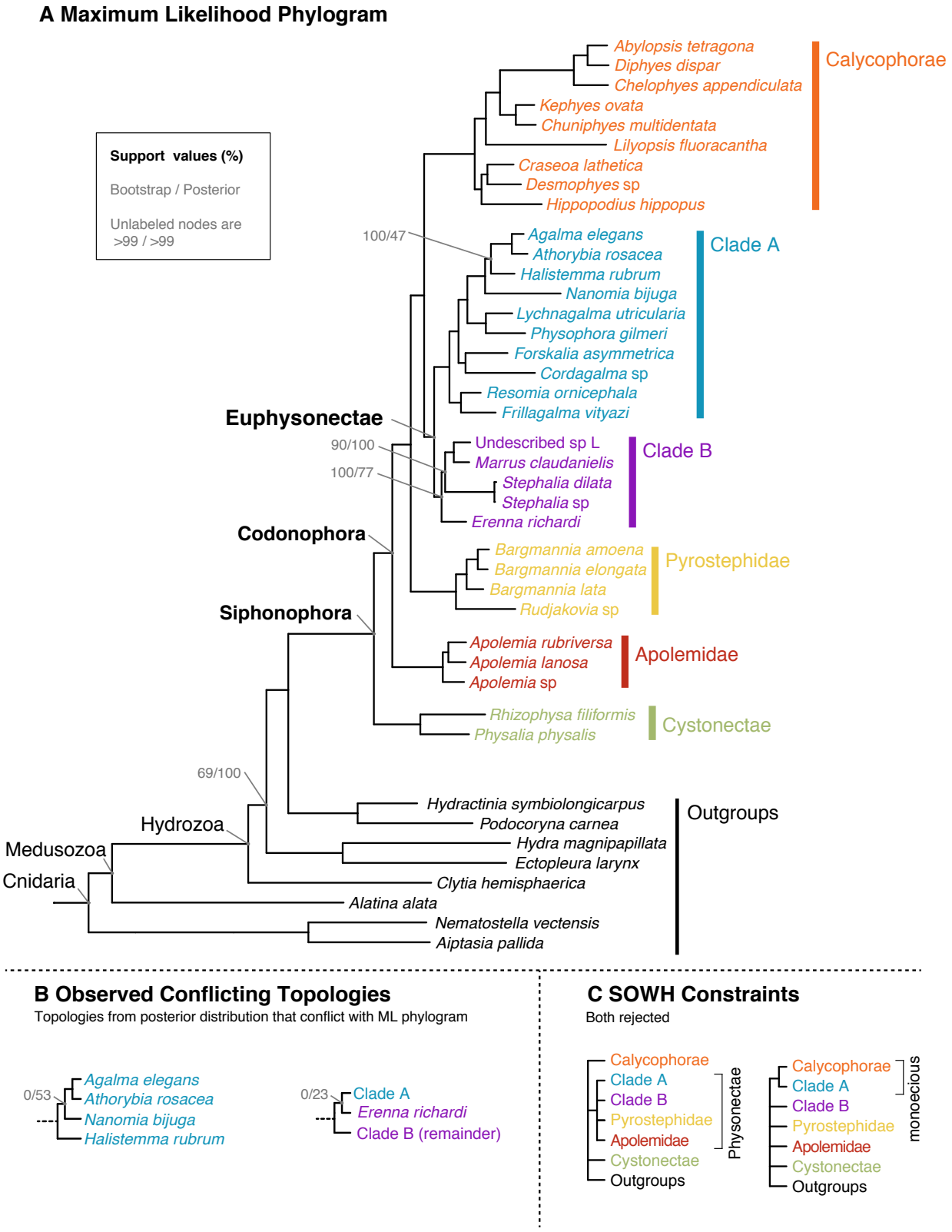

Figure 3: (A) Maximum likelihood (ML) phylogram with bipartation frequencies from the ML bootstraps and the Bayesian posterior distribution of trees. Unlabeled nodes have support >0.99 for both bootstraps and posteriors. (B) The topologies found in the psoterior distribution of trees that conflict with the ML tree. (C) The topologies evaluated by the SOWH tests. For more details on the SOWH topologies refer to Fig. S2.

these species, the male and female zooids are placed at very different but well defined locations within the cormidium. Meanwhile in calycophorans, each cormidium (a single reiterated sequence of zooids along the stem, see Fig. 2) bears either male or female zooids. In this form of monoecy, the male and female cormidia can either be in an alternating pattern, or there can be several male or female cormidia in a row. In either case, male and female zooids are found at the same corresponding locations within the cormidia. However, there are exceptions – in *Sulculeolaria* (not included in this phylogeny), colonies appear to consist of only one sex, however they are monoecious and protoandrous, with female gonophores developing after the release of male gonophores (Carre, 1979).

The Evolution of Zooid Types

One of the most striking aspects of siphonophore biology is their diversity of unique zooid types (Beklemishev, 1969; Cartwright and Nawrocki, 2010). For example, members of *Forskalia* have 5 basic zooid types (nectophore, gastrozooid, palpon, bract, and gonophore), and in some species, a total of 9 when considering zooid subtypes (4 types of bract, male & female gonophores)(Pugh, 2003). Here we reconstruct the evolutionary origins of several zooid types on the present transcriptome tree (Fig. 4).

Nectophores (Fig. 2) are non-reproductive propulsive medusae. In Codonophora, the nectophores are localized to a region known as the nectosome (Fig. 2B), which has its own growth zone, and are used for coordinated colony-level swimming. Nectophores are also present within the gonodendra (reproductive structures) of cystonects, and are thought to propel the gonodendra when they detach from the colony (Totton, 1960, 1965). It is not clear whether the nectophores found within the siphosome of the cystonects are homologous to the nectophores borne on the nectosome of codonophorans. Similarly, the homology of the special nectophore associated with gonophores of the calycophoran *Stephanophyes superba* is also unclear (Chun, 1891). As such, we only consider the evolution of the nectosome in this study, and not the presence/absence of nectophores. The present analyses, as well as the analyses of Dunn et al. (2005), are consistent with a single origin of the nectosome (Fig. S5).

Within the nectosome, the nectophores can be attached along the dorsal or ventral side of the stem, following the orientation framework of Haddock et al. (2005). Our ancestral reconstructions for this character (Fig. S8) suggest that ventral attachment of nectophores was the ancestral state in Codonophora, and that dorsal attachment has independently evolved twice – once along the Agalmatidae stem and once along the Pyrostephidae stem.

Bracts are highly reduced zooids unique to siphonophores, where they are only present in Codonophora (Fig. 4). Bracts are functional for protection of the delicate zooids and to help maintain neutral buoyancy (Jacobs, 1937). Some calycophorans are able to actively exclude sulphate ions in their bracts to adjust their buoyancy along the colony (Bidigare and Biggs, 1980). Bracts were lost in Hippopodidae, some clausophyids, *Physophora hydrostatica*, and in *Gymnopraia lapislazula*. These patterns of loss are not captured by the present sampling, as most of these species are not included in the present phylogeny.

Palpons are modified reduced gastrozooids used for digestion and circulation of the gastrovascular fluid (Mackie et al., 1987). We do not distinguish here between gonopalpons (palpons associated with gonodendra, without a tentacle, as in the cystonects) and palpons borne on the stem (typically with a reduced tentacle or palpacle) (Totton, 1965). We reconstruct them as present in the common ancestor of siphonophores (Fig. 5B), retained in most species, but lost three times independently in the branches leading to *Pyrostephidae* (represented here by the genera *Bargmannia* and *Rudjakovia*), in calycophorans, and in *Marrus claudanielis*. Within the calycophorans, one species *Stephanophyes superba* (not included in this phylogeny) has polyp-like zooids that have been described as palpons (Totton, 1965), but the exact identity of this zooid is not clear and needs further morphological examination.

The Gain and Loss of the Pneumatophore

The pneumatophore is a gas filled float located at the anterior end of the colony, which helps the colony maintain its orientation in the water column, and plays a role in flotation in the case of the cystonects

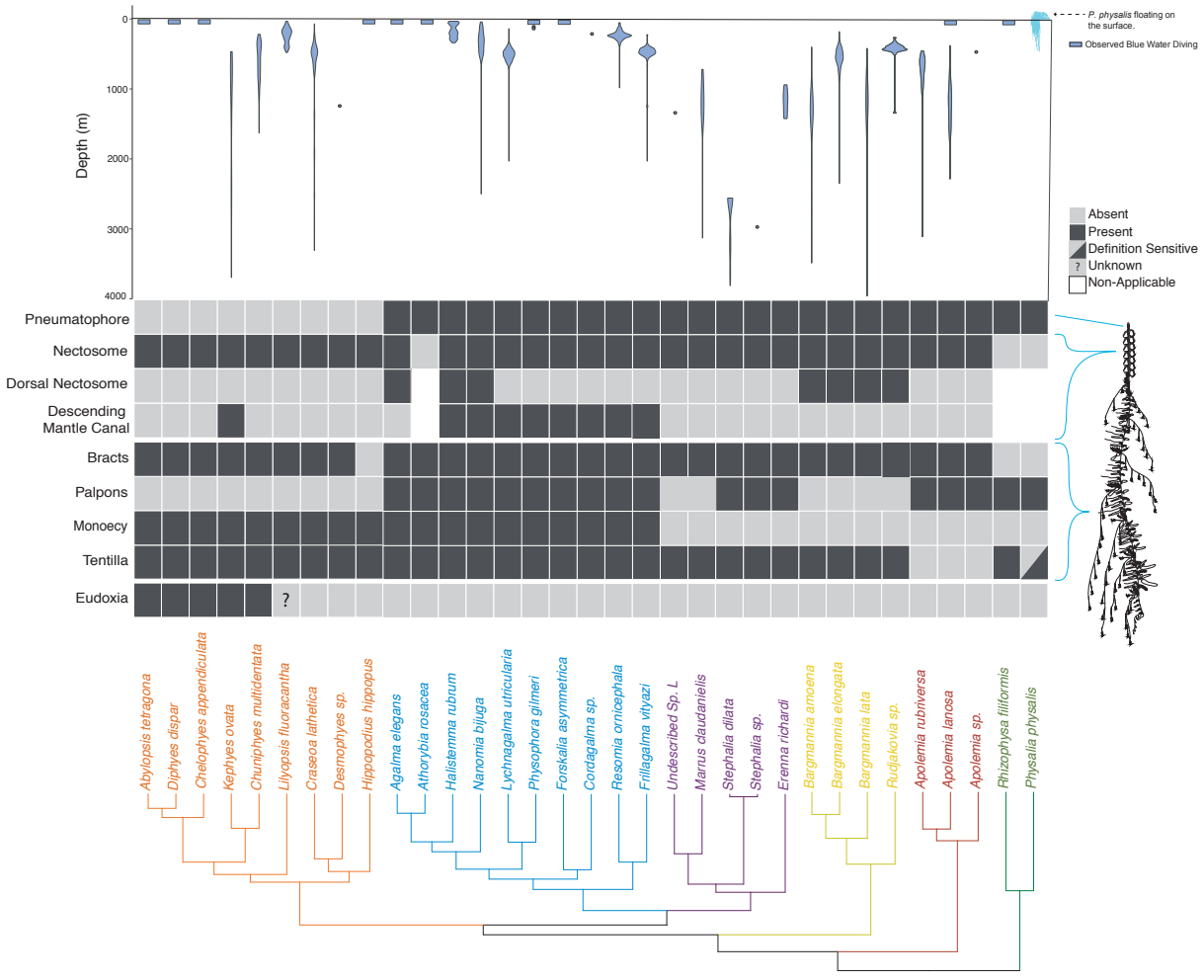

Figure 4: Siphonophore phylogeny showing the distribution of the main anatomical characters and the bathymetric distributions of the different species.

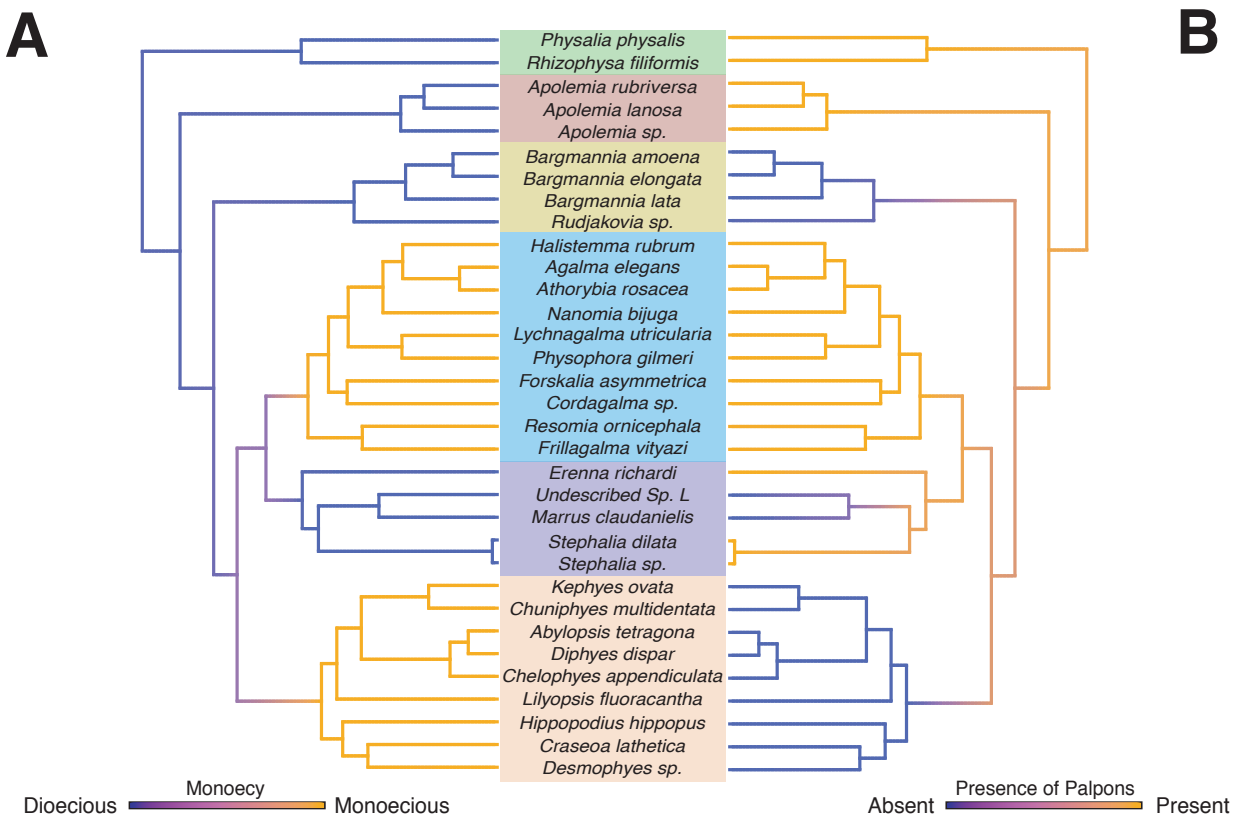

Figure 5: Stochastic mapping reconstruction of the evolutionary history of A) distribution of sexual zooids on the colonies, and B) palpon zooids. The color gradients show the reconstructed probability estimate of the discrete character states along the branches. Intermediate values reflect uncertainty.

(Totton, 1965; Mackie, 1974; Church et al., 2015b). It is not a zooid, as it is not formed by budding but by invagination at the aboral end of the planula during early development (Leloup, 1935; Garstang, 1946; Carré, 1969). Recent descriptions of the neural arrangement in the pneumatophore of *Nanomia bijuga* suggests it could also gather information on relative pressure changes (and thus depth changes), helping regulate geotaxis (Church et al., 2015b). The ancestral siphonophore had a pneumatophore (Fig. 2B), since both cystonects and all "physonects" possess one (Fig. 4). The pneumatophore was lost in Calycophorae and never gained again in that clade. Calycophorans rely on the ionic balance of their gelatinous nectophores and bracts to retain posture and neutral buoyancy (Mackie, 1974).

The Gain and Loss of Tentilla

The most complex nematocyst batteries of Cnidaria are found among the siphonophores. In many siphonophore species these batteries are found in side branches of the tentacle, termed tentilla (Fig. 2A). Outside of Siphonophora, most hydrozoans bear simple tentacles without side branches. It is still an open question whether the common ancestor of Siphonophora had tentilla. The only siphonophores species regarded as lacking tentilla are *Physalia physalis*, *Apolemia* spp., and *Bathyphysa conifera*. Since *B. conifera* is the only member of the *Rhizophysidae* (and of the *Bathyphysa* genus) lacking tentilla, we assume this is a case of secondary loss. When we reconstruct the evolution of this character on the current phylogeny, 70% of simulations support an common ancestor bearing tentilla, with two independent losses leading to *Physalia* and *Apolemia* (Fig. S3). However, this leaves a 30% support for a simple-tentacled common ancestor followed by 2 independent gains of tentilla in the branches leading to *Rhizophysidae* and non-apolemiid codonophorans.

How we define absence of tentilla, especially for *Physalia physalis*, is also important. The tentacles of this species, when uncoiled, show very prominent, evenly spaced, bulging buttons which contain on their ectoderm all active and functionally arranged nematocysts used by the organism for prey capture (Totton, 1960; Bardi and Marques, 2007). Siphonophore tentilla are complete diverticular branchings of the tentacle ectoderm, mesoglea, and gastrovascular canal (lined by endoderm). *Physalia*'s buttons enclose individual fluid-filled chambers connected by narrow channels to the tentacular canal, lined by endoderm (Hessinger and Ford, 1988). This suggests they are not just ectodermal swellings, but probably reduced tentilla. When we define *Physalia physalis* as tentilla bearing, the results for the character reconstruction lead to a more robust support for a tentilla-bearing common ancestor followed by independent losses of tentilla in the branch leading to *Apolemiidae* (Fig. S4), and in *Bathyphysa conifera*.

The Evolution of Vertical Habitat Use

Siphonophores are abundant predators in the pelagic realm, ranging from the surface (*Physalia physalis*) to bathypelagic depths (Figs. 4 and S9) (Mackie et al., 1987; Mapstone, 2014). The depth distribution of siphonophore populations is not always static, as some species are known to be vertical migrators, although this is within a relatively narrow depth range (<100m) (Pugh, 1984). Some species such as *Nanomia bijuga* exhibit synchronous diel migration patterns (Barham, 1966). Using the present phylogeny, we reconstructed the median depth changes along the phylogeny under a Brownian Motion model (Fig. S9), which had the strongest AICc support (compared to non-phylogenetic distributions, and to Ohrnstein-Uhlenbeck). This model indicates a mesopelagic most recent common ancestor, with several independent transition events to epipelagic (light blue) and bathypelagic (dark blue) waters. There was only a single transition to benthic lifestyle on the branch of *Rhodaliidae*, and a single transition to a pleustonic lifestyle on the branch of *Physalia physalis*. Depth appears to be phylogenetically conserved in Euphysonectae after the split between Clade A (shallow living species) and Clade B (deep dwelling species); however several shallow-living species that likely belong in Clade B were not included in this analysis, suggesting that depth may be more labile than it appears. Phylogenetic conservatism is also observed for the mesopelagic Apolemiidae and Pyrostephidae clades, but not for the Calycophorae, which show a diversified evolutionary trajectory for depth. The present sampling, however, is not sufficient to capture significant variation in depth distributions between closely related species. Previous studies have shown that many species that are collected at the same locality are

found to occupy discrete, largely non-overlapping depth distributions, including between species that are closely related (Pugh, 1974).

This reconstruction (Fig. S9) only included species recorded using an ROV, thus it excludes many other independent colonizations of the epipelagic habitat. The ROV observations are reliable below 200m, and no quantative measurements were made on SCUBA dives. Species such as *Hippopodius hippopus*, *Athorybia rosacea*, *Diphyes dispar*, and *Chelophyes appendiculata* are often encountered blue water diving less than 20m from the surface (Fig. 4). We also reconstructed the median depth changes along the phylogeny using median depths of 20m for all species collected by SCUBA diving or swimming (Fig. S10), and still find support for a mesopelagic ancestor. It is important to note, however, that *H. hippopus* and *C. appendiculata* were both collected in the bay of Villefrance-sur-mer, France, where an upwelling is known to bring deeper species closer to the surface (Nival et al., 1976).

Conclusions

Using phylogenomic tools we were able to resolve deep relationships within Siphonophora with strong support. A previous rRNA study was unable to resolve deep relationships within Codonophora, while our study suggests that Pyrostephidae are sister to all other non-apolemiid codonophorans. We find support for two monophyletic groups within the clade that is sister to Pyrostephidae – Calycophorae and a new clade we name Euphysonectae. Within Euphysonectae, we find support for two monophyletic groups dubbed Clade A and Clade B. Our study supports the rejection of the monophyly of Physonectae, a traditional morphological grouping, and rejects the monophyly of monoecious siphonophores. These results are consistent with a hypothesis that monoecy evolved twice, once in Clade A and once in Calycophorae. This hypothesis is consistent with differences in the arrangement of male and female zooids in the two monoecious groups. Future studies with the addition of key taxa within Euphysonectae will enable resolution of internal relationships within Siphonophora, and shed light on patterns of character evolution, including the evolution of zooid types, that cannot be fully assessed here.

Acknowledgements

This work was supported by the National Science Foundation (DEB-1256695 and the Waterman Award). Sequencing at the Brown Genomics Core facility was supported in part by NIH P30RR031153 and NSF EPSCoR EPS-1004057. Data transfer was supported by NSF RII-C2 EPS-1005789. Analyses were conducted with computational resources and services at the Center for Computation and Visualization at Brown University, supported in part by the NSF EPSCoR EPS-1004057 and the State of Rhode Island. SOWHAT analyses were carried out on the Odyssey cluster supported by the FAS Division of Science, Research Computing Group at Harvard University – we thank Cassandra Extavour for use of the Harvard cluster. We thank Rob Sherlock for providing the *Bathyphysa conifera* photograph. We also thank the MBARI crews and ROV pilots for collection of the specimens.

Supplementary Information

Agalma analysis

Stochastic Character maps

```
## [1] 537.7929
## [1] 513.6824
## [1] 516.1099
```

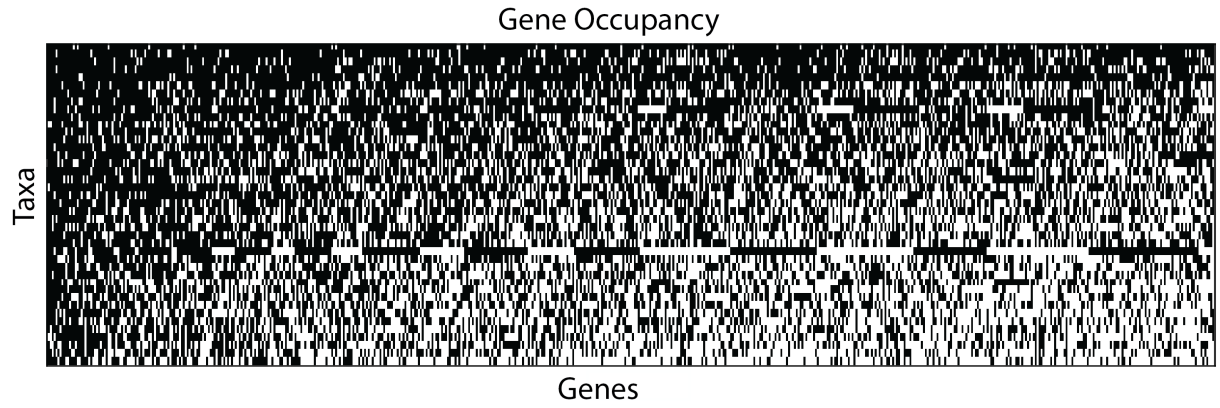

Figure S1: 60% gene occupancy matrix for 41 species across 1,071 genes. Genes and species are sorted by sampling, the best sampled shown in the upper left.

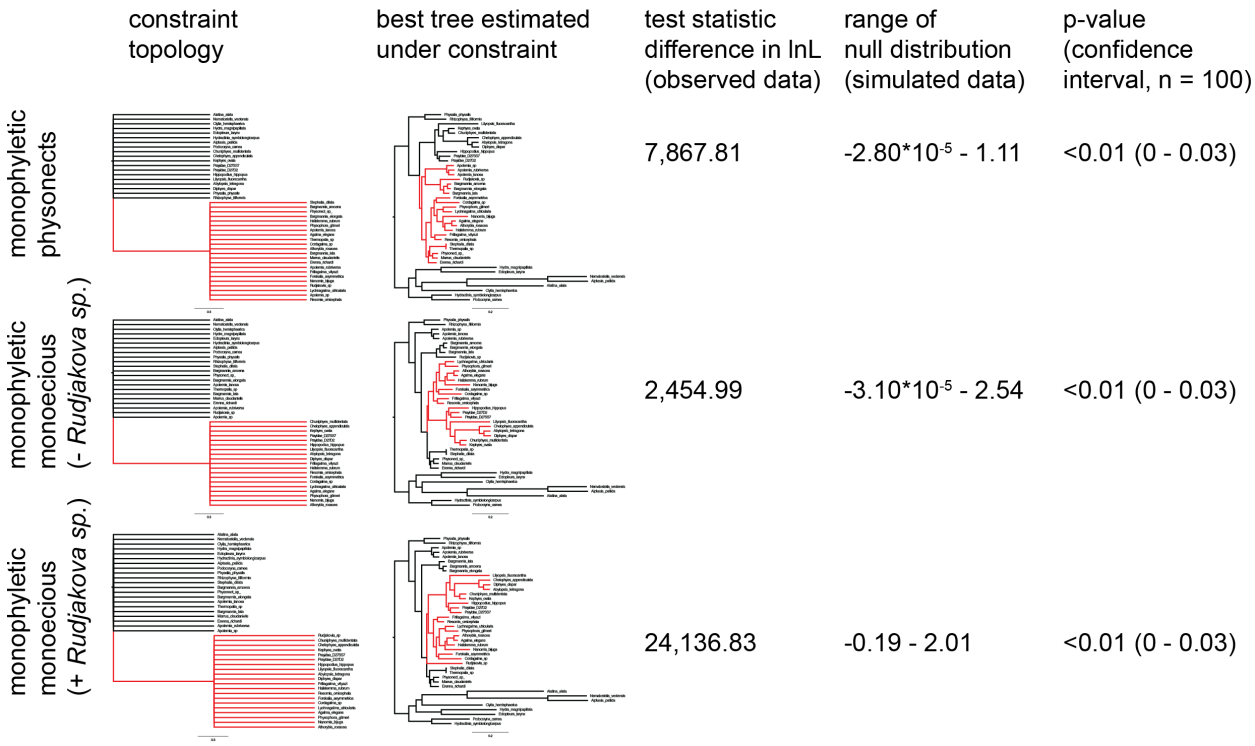

Figure S2: Constrained topologies specified in SOWH testing. Test statistic and p-value for each tree estimated under constraint are given.

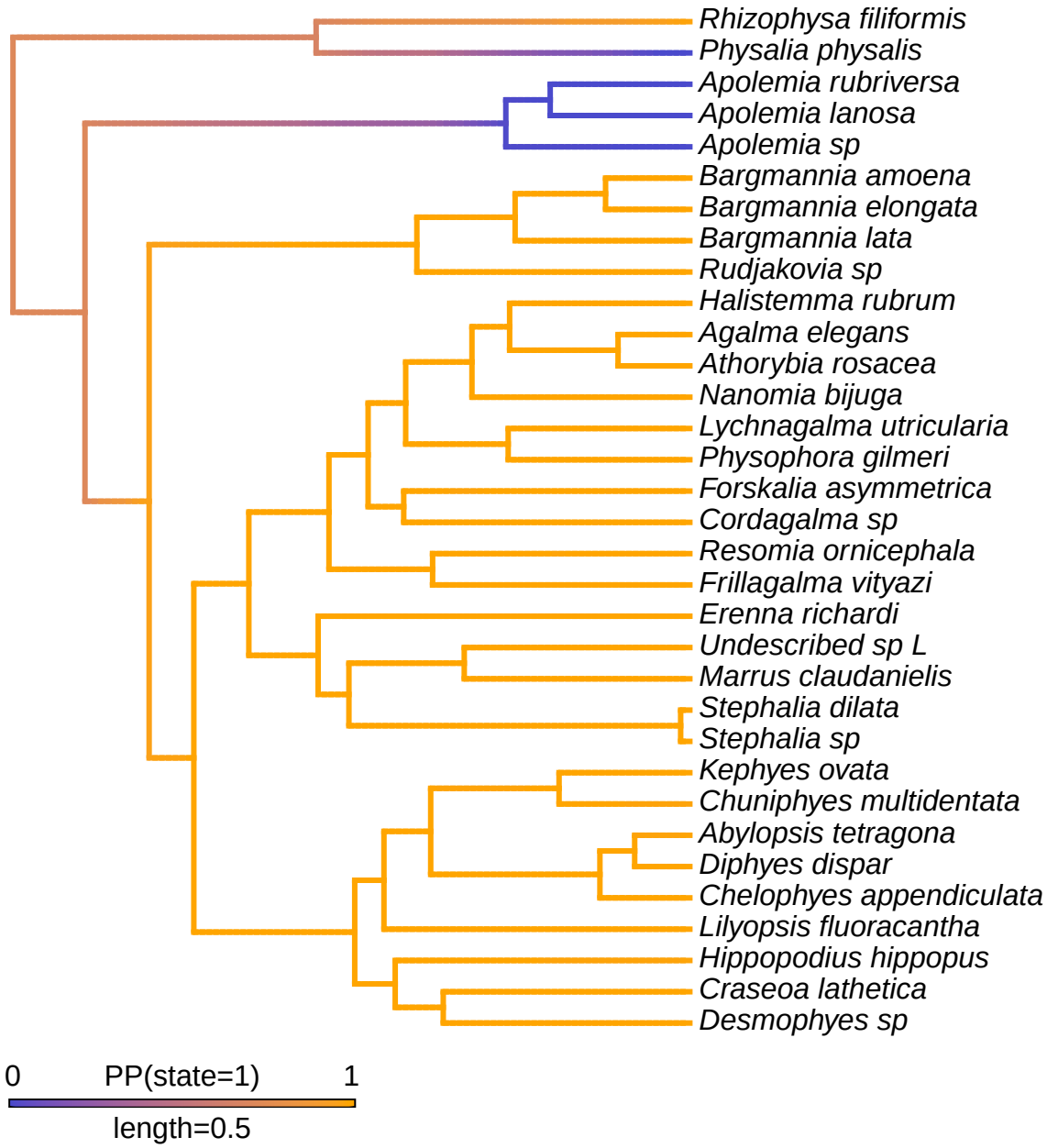

Figure S3: Stochastic character map of presence of tentilla with *Physalia* included as not bearing tentilla.

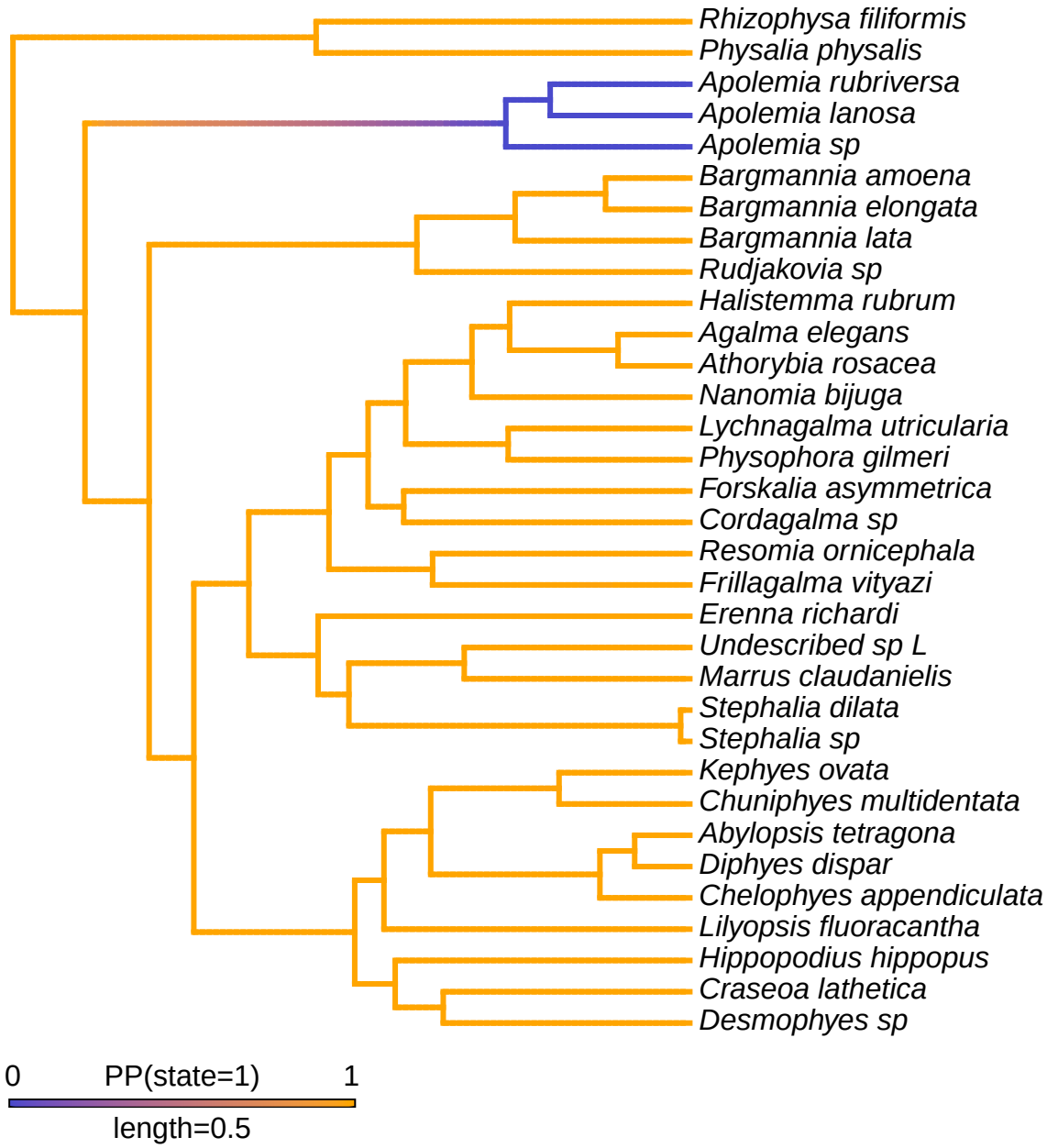

Figure S4: Stochastic character map of presence of tentilla with *Physalia* included as bearing tentilla.

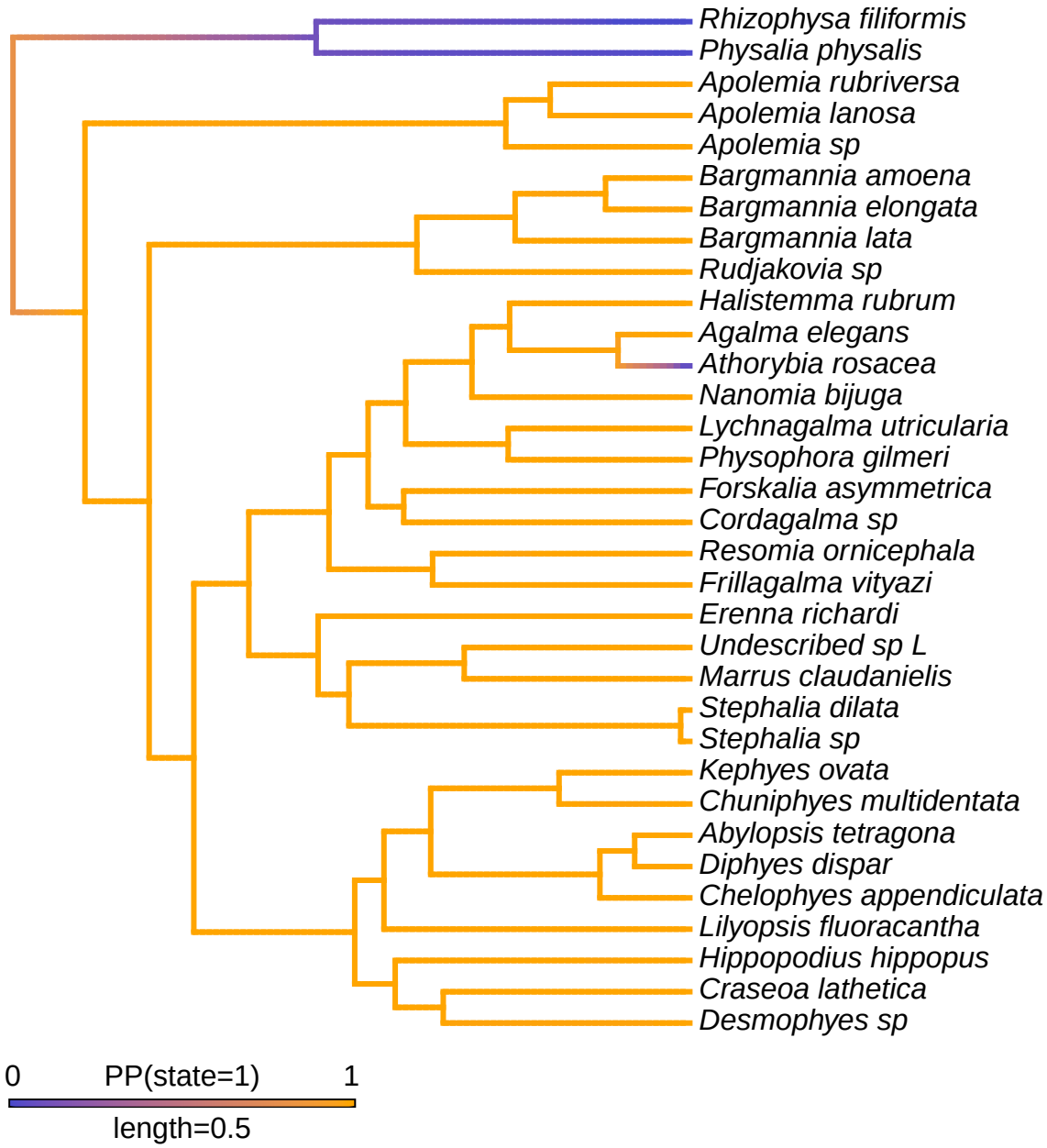

Figure S5: Stochastic character map of presence of nectosome.

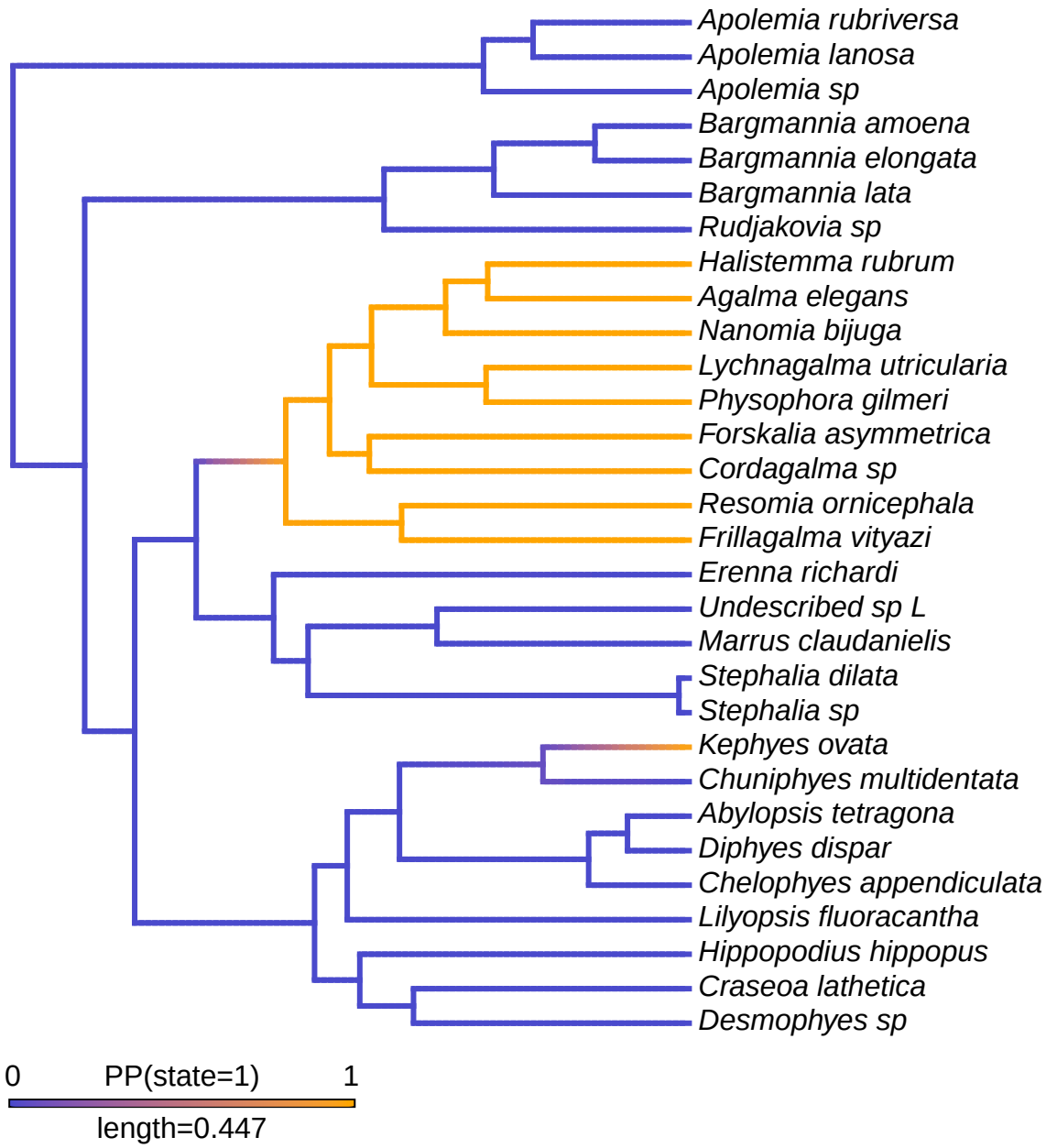

Figure S6: Stochastic character map of presence of a descending mantle canal in the nectophores. Cystonects and Athorybia were excluded as they do not have a nectosome.

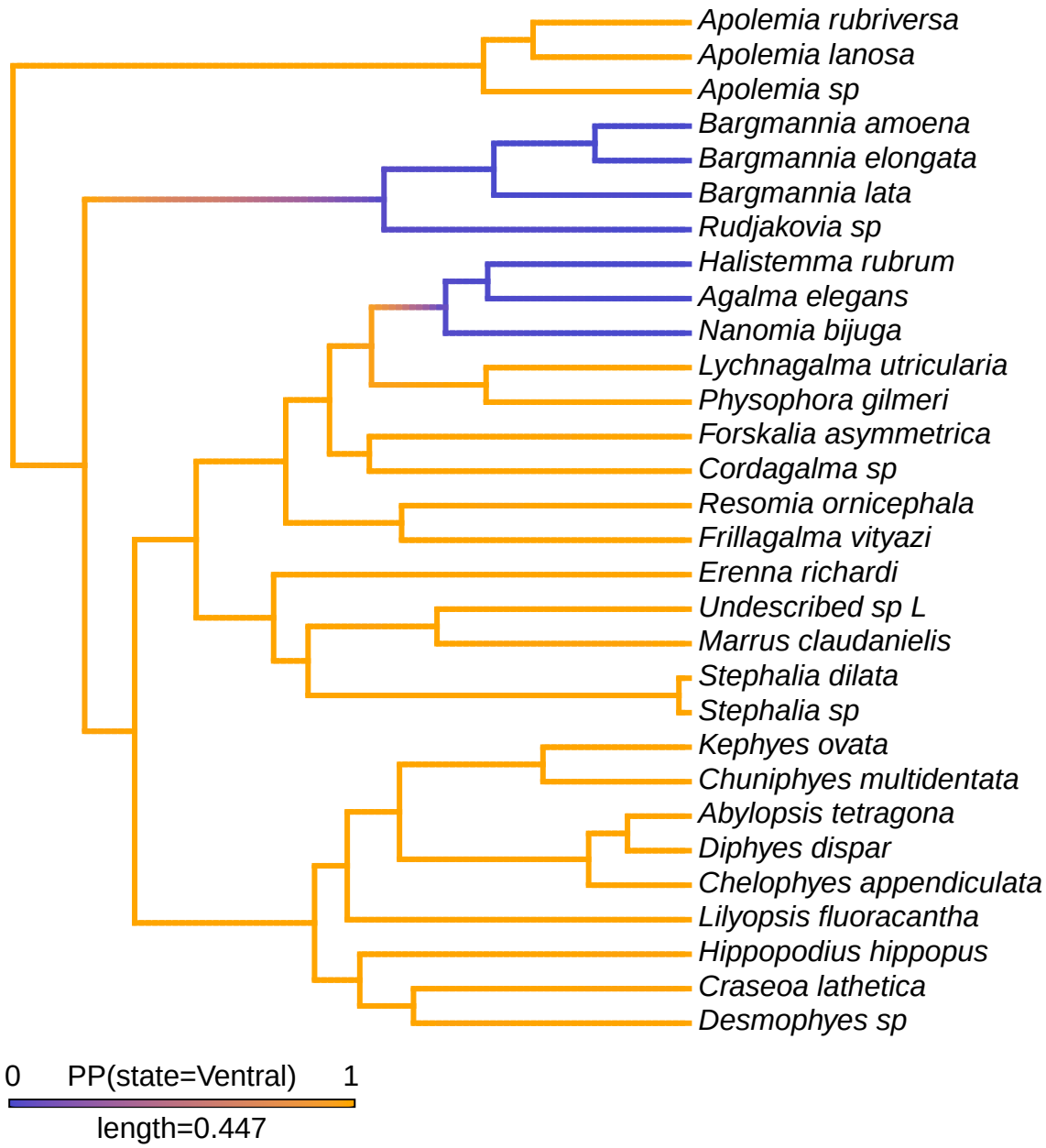

Figure S7: Stochastic character map for the evolution of the position of the nectosome. Cystonects were excluded as they do not have a nectosome.

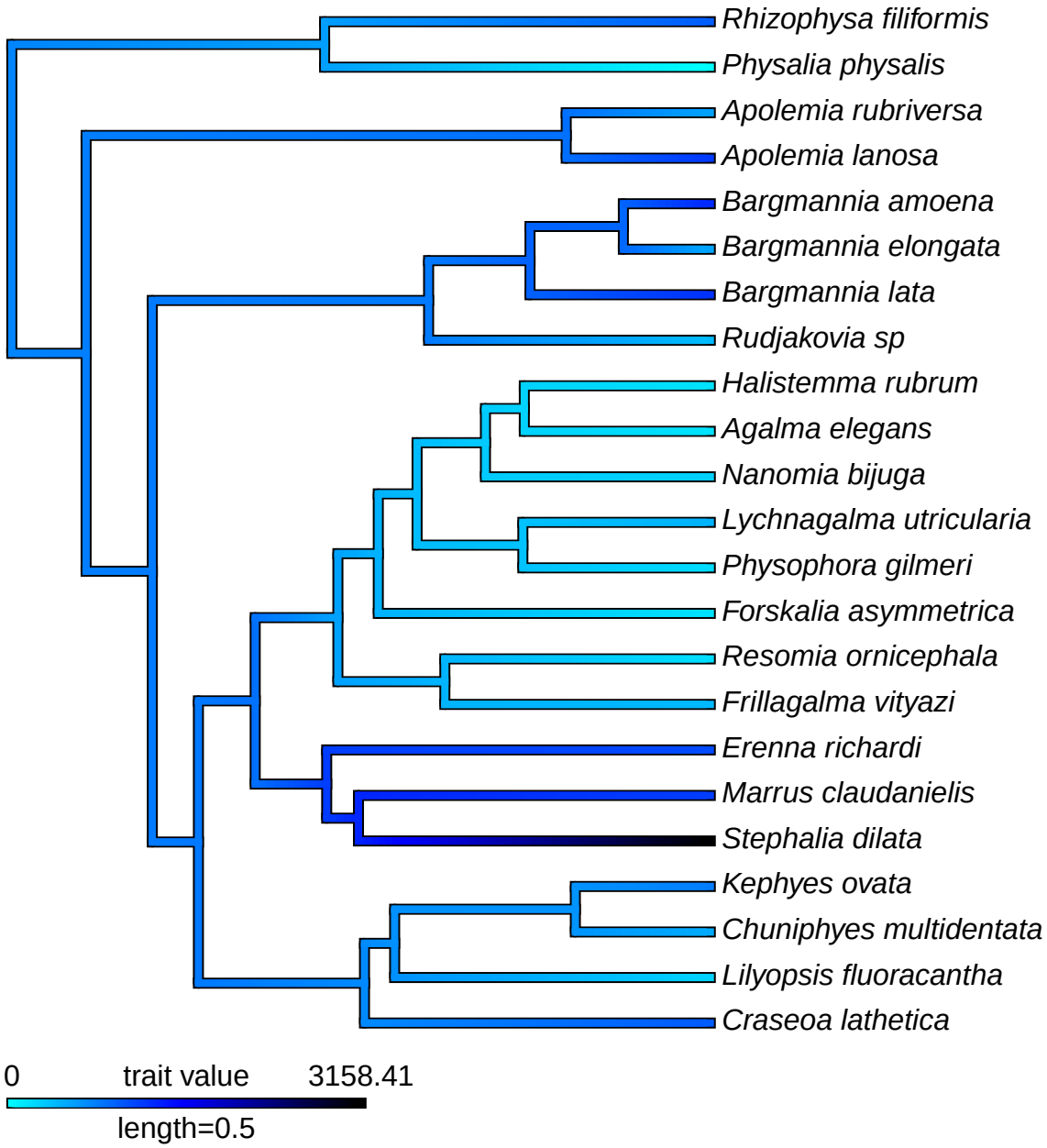

Figure S8: Brownian Motion character map of median depth of species observed with an MBARI ROV.

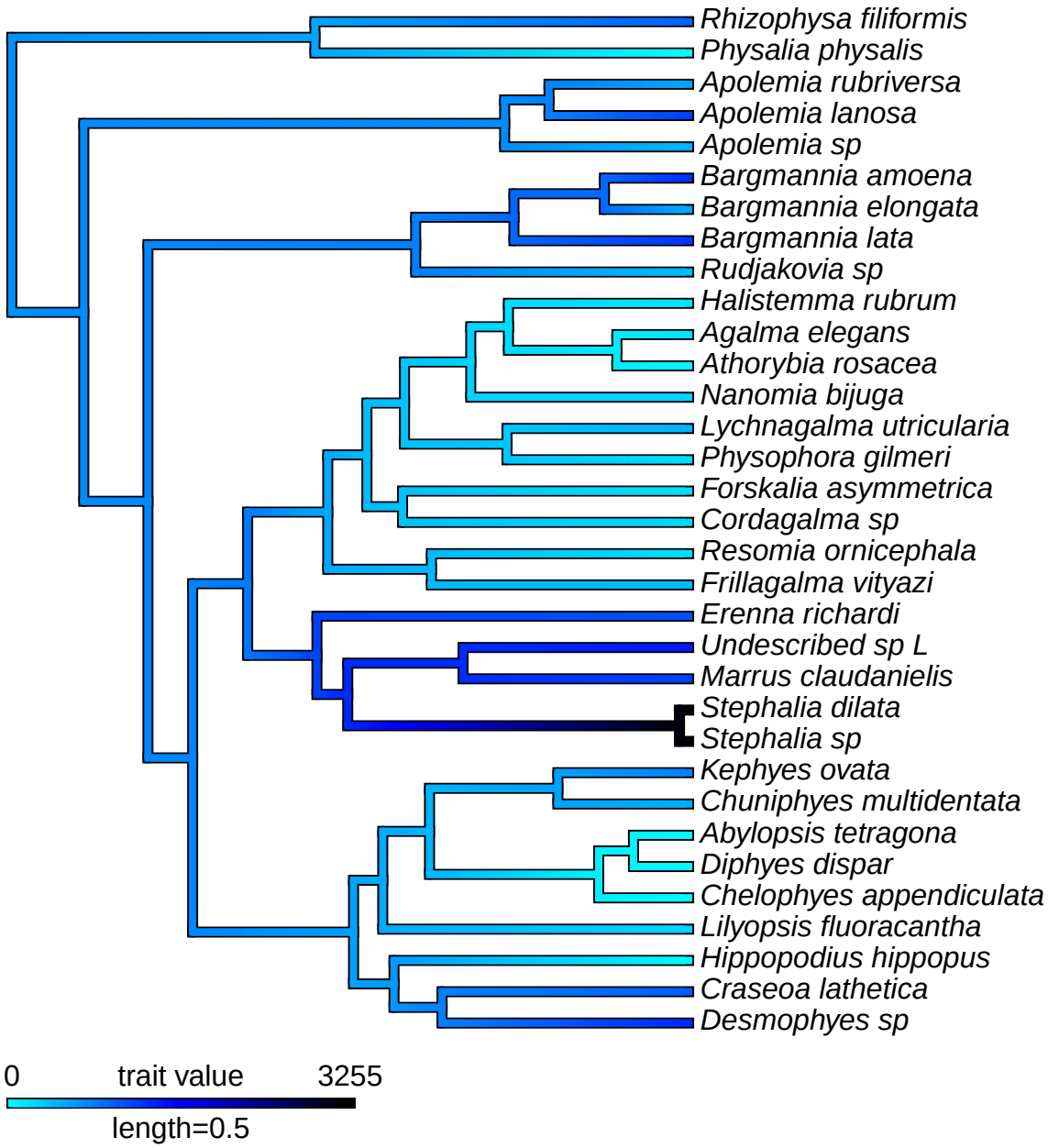

Figure S9: Brownian Motion character map of median depth of species including blue water diving observations.

	K	PICvar obs	PICvar rnd	P-value	Z-score
Nectosome	0.7576982	0.20867575	0.4440476	0.276	-0.5561752
Palpons	2.5304645	0.13420510	1.3926422	0.001	-2.0877019
Tentilla	2.9207926	0.06470251	0.6001549	0.001	-1.1081003
Pneumatophore	3.9936316	0.06932454	1.0841551	0.001	-1.7701531
Bracts	1.8939427	0.08917691	0.4793389	0.001	-0.8714438

Table S1: Phylogenetic signal in the binary traits, including Blomberg's K statistic, the mean observed PIC variance, the random variance of PICs, p-value of the comparison of observed and random variance, and the z-score.

Software versions

This manuscript was computed on Thu Jan 11 13:07:16 2018 with the following R package versions.

```
R version 3.4.1 (2017-06-30)
Platform: x86_64-apple-darwin15.6.0 (64-bit)
Running under: macOS Sierra 10.12.2

Matrix products: default
BLAS: /Library/Frameworks/R.framework/Versions/3.4/Resources/lib/libRblas.0.dylib
LAPACK: /Library/Frameworks/R.framework/Versions/3.4/Resources/lib/libRlapack.dylib

locale:
[1] en_GB.UTF-8/en_GB.UTF-8/en_GB.UTF-8/C/en_GB.UTF-8/en_GB.UTF-8

attached base packages:
[1] grid      parallel  stats     graphics  grDevices utils     datasets
[8] methods   base

other attached packages:
 [1] bindrcpp_0.2     phylolm_2.5      geomorph_3.0.5   rgl_0.98.1
 [5] adephylo_1.1-10  ade4_1.7-8       phylobase_0.8.4  geiger_2.0.6
 [9] phangorn_2.2.0   phytools_0.6-20  picante_1.6-2    nlme_3.1-131
[13] vegan_2.4-4      lattice_0.20-35  permute_0.9-4    ape_4.1
[17] hutan_0.5.0      FactoMineR_1.38  factoextra_1.0.5 gridExtra_2.3
[21] seriation_1.2-2  fields_9.0       maps_3.2.0       spam_2.1-1
[25] dotCall64_0.9-04 ggtree_1.8.2     treeio_1.0.2     cowplot_0.8.0
[29] xtable_1.8-2     jsonlite_1.5     knitr_1.17       digest_0.6.12
[33] magrittr_1.5     forcats_0.2.0    stringr_1.2.0    dplyr_0.7.4
[37] purrr_0.2.3      readr_1.1.1      tidyr_0.7.1      tibble_1.3.4
[41] ggplot2_2.2.1    tidyverse_1.1.1

loaded via a namespace (and not attached):
  [1] readxl_1.0.0            uuid_0.1-2
  [3] backports_1.1.1         fastmatch_1.1-0
  [5] plyr_1.8.4              igraph_1.1.2
  [7] lazyeval_0.2.0          sp_1.2-5
  [9] splines_3.4.1           rncl_0.8.2
 [11] foreach_1.4.3           htmltools_0.3.6
 [13] viridis_0.4.0           gdata_2.18.0
 [15] cluster_2.0.6           gclus_1.3.1
 [17] modelr_0.1.1            gmodels_2.16.2
 [19] prettyunits_1.0.2       jpeg_0.1-8
```

```
 [21] colorspace_1.3-2        rvest_0.3.2
 [23] ggrepel_0.7.0           haven_1.1.0
 [25] bindr_0.1               survival_2.41-3
 [27] iterators_1.0.8         glue_1.1.1
 [29] registry_0.3            gtable_0.2.0
 [31] seqinr_3.4-5            kernlab_0.9-25
 [33] prabclus_2.2-6          DEoptimR_1.0-8
 [35] scales_0.5.0            mvtnorm_1.0-6
 [37] DBI_0.7                 Rcpp_0.12.13
 [39] plotrix_3.6-6           viridisLite_0.2.0
 [41] progress_1.1.2          spdep_0.6-15
 [43] flashClust_1.01-2       foreign_0.8-69
 [45] subplex_1.4-1           bold_0.5.0
 [47] mclust_5.3              deSolve_1.20
 [49] stats4_3.4.1            animation_2.5
 [51] htmlwidgets_0.9         httr_1.3.1
 [53] gplots_3.0.1            fpc_2.1-10
 [55] modeltools_0.2-21       pkgconfig_2.0.1
 [57] reshape_0.8.7           XML_3.98-1.9
 [59] flexmix_2.3-14          deldir_0.1-14
 [61] nnet_7.3-12             crul_0.4.0
 [63] tidyselect_0.2.0        labeling_0.3
 [65] rlang_0.1.2             reshape2_1.4.2
 [67] munsell_0.4.3           cellranger_1.1.0
 [69] tools_3.4.1             broom_0.4.2
 [71] evaluate_0.10.1         yaml_2.1.14
 [73] robustbase_0.92-7       caTools_1.17.1
 [75] dendextend_1.5.2        mime_0.5
 [77] whisker_0.3-2           taxize_0.9.0
 [79] adegenet_2.1.0          leaps_3.0
 [81] xml2_1.1.1              compiler_3.4.1
 [83] curl_2.8.1              clusterGeneration_1.3.4
 [85] RNeXML_2.0.7            stringi_1.1.5
 [87] highr_0.6               trimcluster_0.1-2
 [89] Matrix_1.2-11           psych_1.7.8
 [91] msm_1.6.4               LearnBayes_2.15
 [93] combinat_0.0-8          data.table_1.10.4
 [95] bitops_1.0-6            httpuv_1.3.5
 [97] R6_2.2.2                TSP_1.1-5
 [99] KernSmooth_2.23-15      codetools_0.2-15
[101] boot_1.3-20             MASS_7.3-47
[103] gtools_3.5.0            assertthat_0.2.0
[105] rprojroot_1.2           mnormt_1.5-5
[107] diptest_0.75-7          mgcv_1.8-22
[109] expm_0.999-2            hms_0.3
[111] quadprog_1.5-5          coda_0.19-1
[113] class_7.3-14            rmarkdown_1.6
[115] rvcheck_0.0.9           shiny_1.0.5
[117] numDeriv_2016.8-1       scatterplot3d_0.3-40
[119] lubridate_1.6.0
```

References

Altschul S.F., Gish W., Miller W., Myers E.W., Lipman D.J., 1990. Basic local alignment search tool. Journal of molecular biology. 215, 403–410.

Bardi J., Marques A., 2007. Taxonomic redescription of the Portuguese man-of-war, *Physalia physalis* (Cnidaria, Hydrozoa, Siphonophorae, Cystonectae) from Brazil. Iheringia. Série Zoologia. 97, 425–433.

Barham E.G., 1966. Deep scattering layer migration and composition: Observations from a diving saucer. Science. 151, 1399–1403.

Beklemishev W.N., 1969. Principles of comparitive anatomy of invertebrates., Edinburgh:Oliver & Boyd,

Bidigare R.R., Biggs D.C., 1980. The role of sulfate exclusion in buoyancy maintenance by siphonophores and other oceanic gelatinous zooplankton. Comparative Biochemistry and Physiology Part A: Physiology. 66, 467–471.

Carre C., 1979. Sur le genre sulculeolaria blainville, 1834 (siphonophora, calycophorae, diphyidae). Annales de l'Institut Océanographique. 55, 27–48.

Carré C, 1967. Le developpement larvaire d'*Abylopsis tetragona*. Cahiers de Biologie Marine. 8, 185–193.

Carré C., Carré D., 1991. A complete life cycle of the calycophoran siphonophore *Muggiaea kochi* (Will) in the laboratory, under different temperature conditions: ecological implications. Philosophical Transactions of the Royal Society of London B: Biological Sciences. 334, 27–32.

Carré C., Carré D., 1995. Traité de zoologie. anatomie, systématique, biologie. 523–596.

Carré D., 1969. Etude histologique du developpement de *nanomia bijuga* (chiaje, 1841), siphonophore physonecte, agalmidae. Cahiers de Biologie Marine. 10, 325–341.

Cartwright P., Evans N.M., Dunn C.W., Marques A., Miglietta M.P., Schuchert P., Collins A.G., 2008. Phylogenetics of Hydroidolina (Hydrozoa: Cnidaria). Journal of the Marine Biological Association of the United Kingdom. 88, 1663.

Cartwright P., Nawrocki A.M., 2010. Character evolution in Hydrozoa (phylum Cnidaria). Integrative and Comparative Biology. 50, 456–472.

Choy C.A., Haddock S.H.D., Robison B.H., 2017. Deep pelagic food web structure as revealed by in situ feeding observations. Proceedings of the Royal Society of London B: Biological Sciences. 284,.

Chun C., 1891. Die canarischen siphonophoren i. *stephanophyes superba* und die familie der stephanophyiiden. Abhandlungen herausgegeben von der Senckenbergischen Naturforschenden Gesellschaft. 16, 553–627.

Church S.H., Ryan J.F., Dunn C.W., 2015a. Automation and evaluation of the sowh test with sowhat. Systematic Biology. 64, 1048–1058.

Church S.H., Siebert S., Bhattacharyya P., Dunn C.W., 2015b. The histology of *Nanomia bijuga* (Hydrozoa: Siphonophora). Journal of Experimental Zoology Part B: Molecular and Developmental Evolution. 324, 435–449.

Dunn C., Pugh P., Haddock S., 2005. Molecular Phylogenetics of the Siphonophora (Cnidaria), with Implications for the Evolution of Functional Specialization. Systematic biology. 54, 916–935.

Dunn C.W., Howison M., Zapata F., 2013. Agalma: an automated phylogenomics workflow. BMC Bioinformatics. 14, 330.

Dunn C.W., Wagner G.P., 2006. The evolution of colony-level development in the Siphonophora (Cnidaria: Hydrozoa). Development genes and evolution. 216, 743–754.

Enright A.J., Van Dongen S., Ouzounis C.A., 2002. An efficient algorithm for large-scale detection of protein

families. Nucleic Acids Research. 30, 1575–1584.

Garstang W., 1946. The morphology and relations of the Siphonophora. QJ Microsc. Sci. 87, 103–193.

Grabherr M.G., Haas B.J., Yassour M., Levin J.Z., Thompson D.A., Amit I., Adiconis X., Fan L., Raychowdhury R., Zeng Q., others, 2011. Full-length transcriptome assembly from rna-seq data without a reference genome. Nature biotechnology. 29, 644–652.

Guang A., Howison M., Zapata F., Lawrence C.E., Dunn C., 2017. Revising transcriptome assemblies with phylogenetic information in agalma 1.0. bioRxiv.

Haddock S.H., Dunn C.W., Pugh P.R., 2005. A re-examination of siphonophore terminology and morphology, applied to the description of two new prayine species with remarkable bio-optical properties. Journal of the Marine Biological Association of the United Kingdom. 85, 695–707.

Hessinger D., Ford H., 1988. The Biology of Nematocysts., Academic Press, San Diego.

Huelsenbeck J.P., Nielsen R., Bollback J.P., 2003. Stochastic mapping of morphological characters. Systematic Biology. 52, 131–158.

Jacobs W., 1937. Beobachtungen über das Schweben der Siphonophoren. Journal of Comparative Physiology A: Neuroethology, Sensory, Neural, and Behavioral Physiology. 24, 583–601.

Katoh K., Standley D.M., 2013. MAFFT multiple sequence alignment software version 7: Improvements in performance and usability. Molecular biology and evolution. 30, 772–780.

Langmead B., Salzberg S.L., 2012. Fast gapped-read alignment with bowtie 2. Nature methods. 9, 357–359.

Lartillot N., Lepage T., Blanquart S., 2009. PhyloBayes 3: a Bayesian software package for phylogenetic reconstruction and molecular dating. Bioinformatics. 25, 2286–2288.

Lartillot N., Philippe H., 2004. A bayesian mixture model for across-site heterogeneities in the amino-acid replacement process. Molecular Biology and Evolution. 21, 1095–1109.

Leloup E., 1935. Les siphonophores de la rade de Villefranche-sur-Mer (Alpes Maritimes, France). Bulletin de Musée Royal d'Histoire Naturelle de Belgique. 11, 1–12.

Li B., Dewey C.N., 2011. RSEM: Accurate transcript quantification from rna-seq data with or without a reference genome. BMC bioinformatics. 12, 323.

Li H., Handsaker B., Wysoker A., Fennell T., Ruan J., Homer N., Marth G., Abecasis G., Durbin R., 2009. The sequence alignment/map format and samtools. Bioinformatics. 25, 2078–2079.

Mackie G., 1974. Locomotion, flotation, and dispersal., Academic Press, New York, USA,

Mackie G., Pugh P., Purcell J., 1987. Siphonophore biology. Advances in marine biology. 24, 97–262.

Mapstone G.M., 2014. Global diversity and review of Siphonophorae (Cnidaria: Hydrozoa). PLoS One. 9, e87737.

Nival P., Gostan J., Malara G., Chara R., 1976. Evolution du plancton dans la baie de villefranche-sur-mer ala fin du printemps (mai et juin 1971), 2. biomasse de phytoplancton et production primarie. Vie Milieu. 26, 47–76.

Pagès F., González H., Ramón M., Sobarzo M., Gili J.-M., 2001. Gelatinous zooplankton assemblages associated with water masses in the Humboldt Current System, and potential predatory impact by Bassia bassensis (Siphonophora: Calycophorae). Marine Ecology Progress Series. 210, 13–24.

Pugh P., 1974. The vertical distribution of the siphonophores collected during the sond cruise, 1965. Journal of the Marine Biological Association of the United Kingdom. 54, 25–90.

Pugh P., 1983. Benthic Siphonophores: A Review of the Family Rhodaliidae (Siphonophora, Physonectae). Philosophical Transactions of the Royal Society of London, B. 301, 165–300.

Pugh P., 1984. The diel migrations and distributions within a mesopelagic community in the north east

Atlantic. 7. Siphonophores. Progress in Oceanography. 13, 461–489.

Pugh P., 2003. A revision of the family Forskaliidae (Siphonophora, Physonectae). Journal of Natural History. 37, 1281–1327.

Pugh P., 2006. The taxonomic status of the genus Moseria (Siphonophora, Physonectae). Zootaxa. 1343, 1–42.

Pugh P., 2016. A synopsis of the Family Cordagalmatidae fam. nov.(Cnidaria, Siphonophora, Physonectae). Zootaxa. 4095, 1–64.

Pugh P., Pages F., Boorman B., 1997. Vertical distribution and abundance of pelagic cnidarians in the eastern Weddell Sea, Antarctica. Journal of the marine Biological Association of the United Kingdom. 77, 341–360.

Purcell J., 1981. Dietary composition and diel feeding patterns of epipelagic siphonophores. Marine Biology. 65, 83–90.

Revell L.J., 2012. Phytools: An r package for phylogenetic comparative biology (and other things). Methods in Ecology and Evolution. 3, 217–223.

Schlining B., Stout N.J., 2006. MBARI's video annotation and reference system. OCEANS 2006. 1–5.

Stamatakis A., 2006. RAxML-vi-hpc: Maximum likelihood-based phylogenetic analyses with thousands of taxa and mixed models. Bioinformatics. 22, 2688–2690.

Sukumaran J., Holder M.T., 2010. DendroPy: A python library for phylogenetic computing. Bioinformatics. 26, 1569–1571.

Swofford D., Olsen G., Waddell P., Hillis D., 1996. Molecular systematics. 2nd ed., Sunderland (MA): Sinauer Associates,

Talavera G., Castresana J., 2007. Improvement of phylogenies after removing divergent and ambiguously aligned blocks from protein sequence alignments. Systematic biology. 56, 564–577.

Totton A., 1960. Studies on *Physalia physalis* (L.). Part 1. Natural history and morphology. Discovery Reports. 30, 301–368.

Totton A.K., 1965. A synopsis of the Siphonophora., British Museum (Natural History),

Williams R., Conway D., 1981. Vertical distribution and seasonal abundance of Aglantha digitale (OF Müller)(Coelenterata: Trachymedusae) and other planktonic coelenterates in the northeast Atlantic Ocean. Journal of Plankton Research. 3, 633–643.

Yu G., Smith D.K., Zhu H., Guan Y., Lam T.T.-Y., 2016. ggtree: an r package for visualization and annotation of phylogenetic trees with their covariates and other associated data. Methods in Ecology and Evolution. 8, 28–36.

Zapata F., Goetz F.E., Smith S.A., Howison M., Siebert S., Church S.H., Sanders S.M., Ames C.L., McFadden C.S., France S.C., others, 2015. Phylogenomic analyses support traditional relationships within Cnidaria. PLoS One. 10, e0139068.